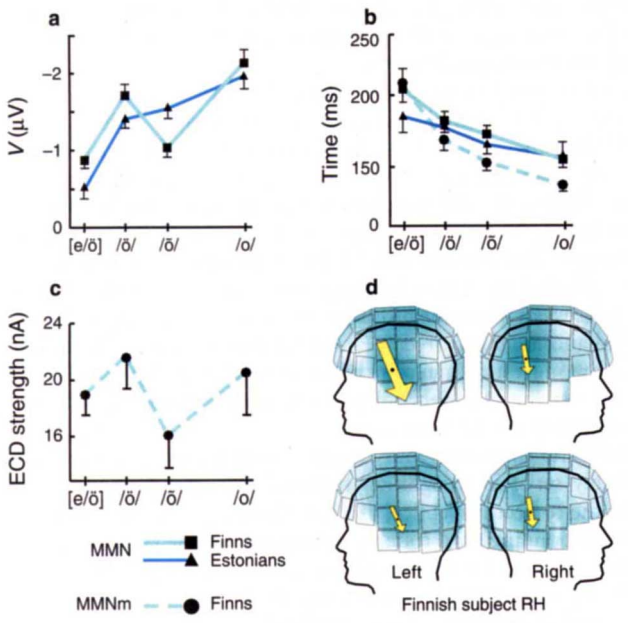

Figure 4 a, MMN peak amplitude (at Fz) in Finns (blue) and Estonians (purple) as a function of the deviant stimulus, arranged in the order of increasing F2 difference from the standard stimulus. Bars indicate s.e.m. **b**, MMN (at Fz) (solid lines) and MMNM (left hemisphere) (broken line) peak latencies as a function of the deviant stimulus for Finns (blue) and Estonians (purple). **c**, Strength of the equivalent current dipole (ECD; average of 9 Finnish subjects) modelling the left auditory-cortex MMNM for the different deviant stimuli. **d**, Left- and right-hemisphere MMNMs of one typical Finnish subject for deviants /ö/ and /õ/ presented in contour (spacing 2 fT cm^{-1}) maps of the magnetic field-gradient amplitude at the MMNM peak latency. The squares indicate the arrangement of the magnetic sensors. The arrows represent ECDs indicating activity in the auditory cortex; the black dots in these arrows show the centres of gravity of MMNM. Note that the prototype /ö/ elicits a much larger MMNM in the left than in the right hemisphere, whereas non-prototype /õ/ responses in both hemispheres are small and quite similar in amplitude.

the vocal tract, and the lip-radiation effect[22]. In this way we could accurately adjust the formants of the stimuli without making sound quality too artificial. The excitation process was computed from a male voice (vowel /a/, normal phonation) using an automatic inverse filtering technique[23]. The vocal tract was modelled using an eighth-order all-pole filter with coefficients adjusted to shift the second formant. The lip-radiation effect was modelled with a fixed differentiator.

Behavioural task. The stimuli, presented at 1,400-ms onset-to-onset intervals, were 75 dB in intensity and 400 ms in duration (with rise and fall times of 10 ms each). Each stimulus was presented about 30 times. Finnish subjects were instructed to press the /e/, /ö/ or /o/ button when the stimulus sounded as a good representative of that category. For Estonians, there was also a response button for their /õ/.

Electric measurements. Measurements were performed in an acoustically and electrically shielded room. Blocks of the vowel /e/ were binaurally presented (75 dB, with a duration of 400 ms including 10-ms rise and fall times) through headphones as the standard stimuli, 15% of the stimuli were randomly appearing deviant sounds (one type per block). The onset-to-onset inter-stimulus interval was 900 ms. The nose-referenced electroencephalogram (EEG, sampling rate 250 Hz) was averaged and digitally filtered (passband 1–30 Hz). Epochs with artefacts exceeding 100 μV at any electrode or with an electro-oculogram (EOG) response exceeding 150 μV were discarded. The baseline for the waveforms was defined as the mean amplitude between −50 and 0 ms relative to stimulus onset. The MMN amplitude was determined from the Fz electrode (where it was usually largest) separately for each subject as the mean amplitude of the 150-ms period centred at the largest peak between 100 and 240 ms.

Magnetic measurements. The experimental paradigm was the same as for the electric measurements. The magnetic responses were measured using a helmet-shaped, whole-head Neuromag-122 magnetometer[24] (sampling rate 397 Hz). The stimuli were delivered through plastic tubes and earpieces at 60 dB above the individual hearing level. Epochs with an electro-oculogram or magnetoencephalogram change exceeding 150 μV or 1,500 fT cm^{-1}, respectively, were omitted from subsequent analysis. The locus of the neuronal activity was estimated by determining the equivalent current dipole at the MMNM peak latency using 40–44 channels separately over the left and right frontotemporal cortices.

Received 12 August; accepted 2 December 1996.

1. Kuhl, P. K. *Percept. Psychophys.* **50,** 93–107 (1991).
2. Liberman, A. M., Harris, K. S., Hoffman, H. S. & Griffith, B. C. *J. Exp. Psychol.* **54,** 358–368 (1957).
3. Kuhl, P. K. *J. Phonet.* **21,** 125–139 (1993).
4. Näätänen, R., Gaillard, A. W. K. & Mäntysalo, S. *Acta Psychol.* **42,** 313–329 (1978).
5. Näätänen, R. *Ear Hear.* **16,** 6–18 (1995).
6. Näätänen, R. *Attention and Brain Function* (Lawrence Erlbaum, Hillsdale, NJ, 1992).
7. Tiitinen, H., May, P., Reinikainen, K. & Näätänen, R. *Nature* **372,** 90–92 (1994).
8. Aaltonen, O., Eerola, O., Hellström, Å., Unispaikka, E., & Lang, A. H. *J. Acoust. Soc. Am.* (in the press).
9. Aulanko, R., Hari, R., Lounasmaa, O., Näätänen, R., & Sams, M. *NeuroReport* **2,** 1356–1358 (1993).
10. Kraus, N. *et al. Science* **273,** 971–973 (1996).
11. Hari, R. in *Auditory Evoked Magnetic Fields and Electric Potentials. Advances in Audiology* Vol. 6 (eds Grandori, F., Hoke, M. & Romani, G. L.) 222–282 (Karger, Basel, 1990).
12. Hämäläinen, M., Hari, R., Ilmoniemi, R. J., Knuutila, J. & Lounasmaa, O. V. *Rev. Mod. Phys.* **65,** 413–497 (1993).
13. Wiik, K. *Ann. Univ. Turku.* **94,** 1–192 (1965).
14. Iivonen, A. *Phonetica* **52,** 221–224 (1995).
15. Liiv, G. & Remmel, M. *Sov. Fenno-Ugric Studies VI* **1,** 7–23 (1970).
16. Näätänen, R., Ilmoniemi, R. J. & Alho, K. *Trends Neurosci.* **7,** 389–395 (1994).
17. Näätänen, R. & Alho, K. *Electroenceph. Clin. Neurophysiol.* (suppl.) **44,** 179–185 (1995).
18. Kuhl, P. K., Williams, K. A. & Lacerda, F. *Science* **255,** 606–608 (1992).
19. Giard, M. H. *et al. J. Cogn. Neurosci.* **7,** 133–143 (1995).
20. Alho, K. *et al. Psychophysiology* **33,** 369–375 (1996).
21. Levänen, S., Ahonen, A., Hari, R., McEvoy, L. & Sams, M. *Cereb. Cortex* **6,** 288–296 (1996).
22. Fant, G. *The Acoustic Theory of Speech Production* (Mouton, Hague, 1960).
23. Alku, P. *Speech Commun.* **11,** 109–118 (1992).
24. Knuutila, J. E. T. *et al. IEEE Trans. Magnet.* **29,** 3315–3320 (1992).

Acknowledgements. We thank G. Nyman, H. Tiitinen, P. Laurinen, E. Service and J. Kekoni for comments on previous versions of this manuscript, and T. Rinne for technical support. This work was supported by the Academy of Finland.

Correspondence and requests for materials should be addressed to R.N. (e-mail: risto.naatanen@helsinki.fi). Further material, including the sound stimuli, are available at http://www.psych.helsinki.fi/papers/nature3/.

Bcl-2 promotes regeneration of severed axons in mammalian CNS

Dong Feng Chen*†, Gerald E. Schneider†, Jean-Claude Martinou‡ & Susumu Tonegawa*†

*Howard Hughes Medical Institute, Center for Learning and Memory, Center for Cancer Research, and * Departments of * Biology and † Brain and Cognitive Sciences, Massachusetts Institute of Technology, Cambridge, Massachusetts 02139, USA*
‡ Glaxo Institute for Molecular Biology, 14 Chemin des Aulx, plan-les-Ouates, 1228 Geneva, Switzerland

Most neurons of the mammalian central nervous system (CNS) lose the ability to regenerate severed axons *in vivo* after a certain point in development[1]. At least part of this loss in regenerative potential is intrinsic to neurons[2–4]. Although embryonic retinal ganglion cells (RGCs) can grow axons into tectum of any age, most RGCs from older animals fail to extend axons into CNS tissue derived from donors of any age, including the embryonic tectum[2]. Here we report that the proto-oncogene *bcl-2* plays a key role in this developmental change by promoting the growth and regeneration of retinal axons. This effect does not seem to be an indirect consequence of its well-known anti-apoptotic activity. Another anti-apoptotic drug, ZVAD, supported neuronal survival but did not promote axon regeneration in culture. This finding could lead to new strategies for the treatment of injuries to the CNS.

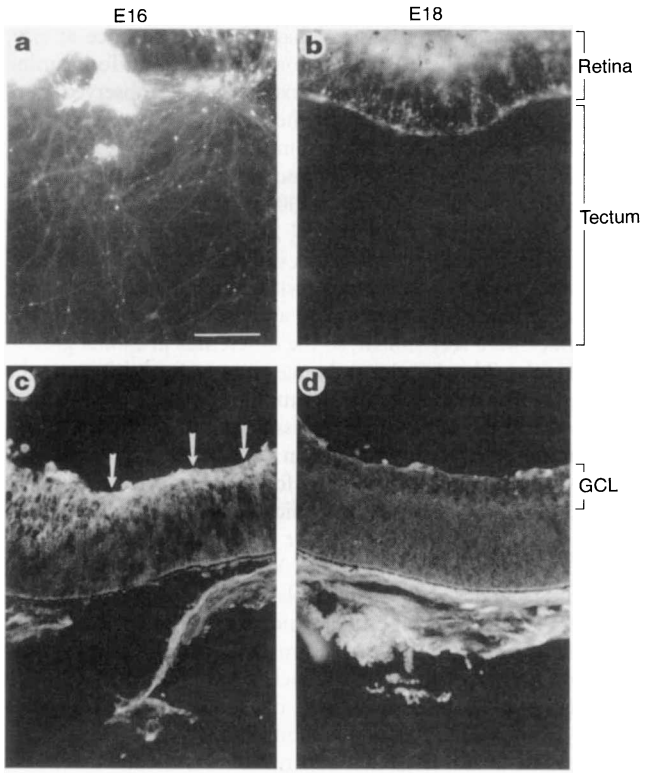

Figure 1 The level of expression of *bcl-2* in RGCs correlates with the growth ability of retinal axons. **a**, **b**, Epifluorescence photomicrographs of DiI-labelled retinal axons in cultures prepared from E16 (**a**) and E18 (**b**) wild-type mice. **c**, **d**, Immunofluorescent staining of Bcl-2 on transverse sections of retinae obtained from E16 (**c**) and E18 (**d**) embryos. Axons from E16 retinae (**a**) can be observed growing into the entire tectal explant; correspondingly, labelling of Bcl-2 appears positive in the retinal ganglion-cell layer (GCL) (**c**). However, the retinal explant derived from E18 animals (**b**) fails to grow axons into the tectal tissue, and the labelling of Bcl-2 disappears from the retinal ganglion-cell layer (**d**). Arrows in **c**, point to the retinal ganglion cell layer with positive labelling. Scale bar, 200 μm.

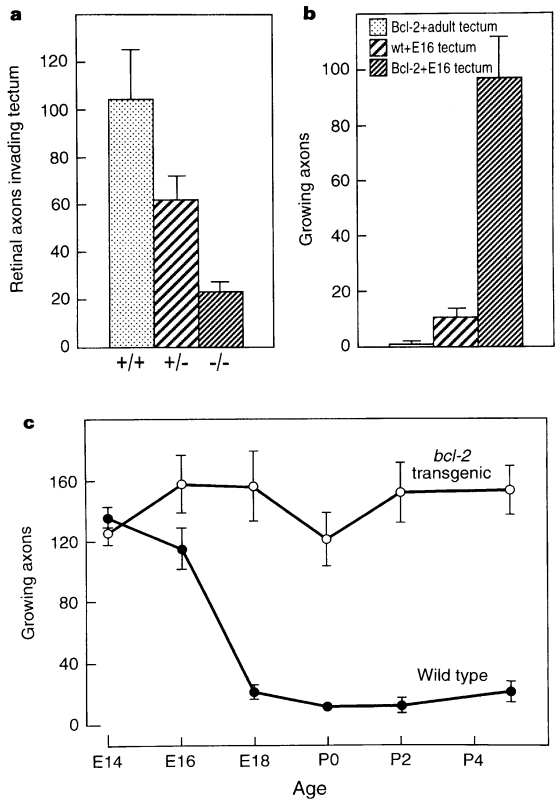

Figure 2 The expression of *bcl-2* is essential for the growth of most retinal axons in culture. Quantification of retinal axon growth observed in cultures from wild-type (C57BL/6J), *bcl-2* null and *bcl-2* transgenic mice. **a**, Quantification of cultures derived from E15 pups genetically deficient in *bcl-2*. Retinal explant derived from heterozygous (+/−) or homozygous (−/−) mutant mice both showed decreased numbers of axons that invaded the tectal tissue when compared with those of wild-type animals (+/+) at this age. **b**, Quantitative results for the growth of retinal axons from adult retinae. Retinal explants derived from adult transgenic mice display 10-fold more axonal growth into E16 tectum than seen retinal explants from wild-type mice. **c**, Growth curves of retinal axons obtained from retinotectal co-cultures, using tissues from wild-type or transgenic animals aged E14 to P5. Note that at age E18 or older there is a marked decrease in numbers of retinal axons from wild-type animals. This decline was not observed for *bcl-2* transgenic mice.

To examine the growth of CNS axons of mice, we established an organotypic co-culture model of the retinotectal system in which the growth pattern of retinal axons closely mimics that seen *in vivo*[2]. Tissues from retinae and midbrain tecta of C57BL/6J mice were abutted in a culture well. Quantitative analysis of axonal growth from retinae was achieved by standard placement of four DiI crystals into each retinal explant. We first examined co-cultures prepared from animals aged embryonic day 14 (E14, where E0 was the day of mating) to E16. Growth of retinal axons into the tectal slice was extensive ($n = 20$) (Figs 1 and 2). The number of labelled axons invading tectal tissue averaged 126 ± 10.0. In contrast, retinal explants ($n = 60$) prepared from animals at age E18 and older exhibited markedly reduced axonal growth. For E18 tissue, the mean number in the labelled sample was 15.5 ± 3.3 fibres per tectal slice (Figs 1b and 2c). This indicated that, starting at E18 in mice, most RGC axons fail to regenerate in culture. These findings are similar to those previously reported on the Syrian hamster[2].

To examine whether the observed age-dependent reduction in the growth of retinal axons is due to increased RGC death, we counted the dying cells in retinal explants, using Sytox green fluorescent dead-cell stain. There were 121 ± 21 cells mm^{-2} ($n = 4$) and 138 ± 19 cells mm^{-2} ($n = 3$) for E16 and E18 retinal explants, respectively, indicating that there was no significant increase in cell death before and after the regenerative failure occurred. We also counted the cells in the RGC layer, and found 85.8 ± 1.7 ($n = 3$) and 80.4 ± 2.1 ($n = 3$) cells per 200-μm retinal segment at E16 and E18, respectively. At either age, few pyknotic cells were found in the RGC layer. It has been shown that the prenatal ganglion cell layer comprises almost entirely RGCs[5], so these data suggest that there is no significant change in RGC number between E16 and E18 retinae. Therefore, the observed age-dependent reduction in the growth of retinal axons cannot be attributed to the loss of RGCs.

We have previously shown that the regenerative failure of most of the older axons seems to be controlled by a genetic programme executed in developing neurons[2]. To determine which genes might play such roles in regulating the growth of retinal axons, we compared the level of expression of several molecules, including neural cell adhesion molecule (NCAM), β-amyloid precursor protein and *bcl-2* protein (Bcl-2), with the use of immunofluorescence staining. We found high expression of *bcl-2* at E16 in

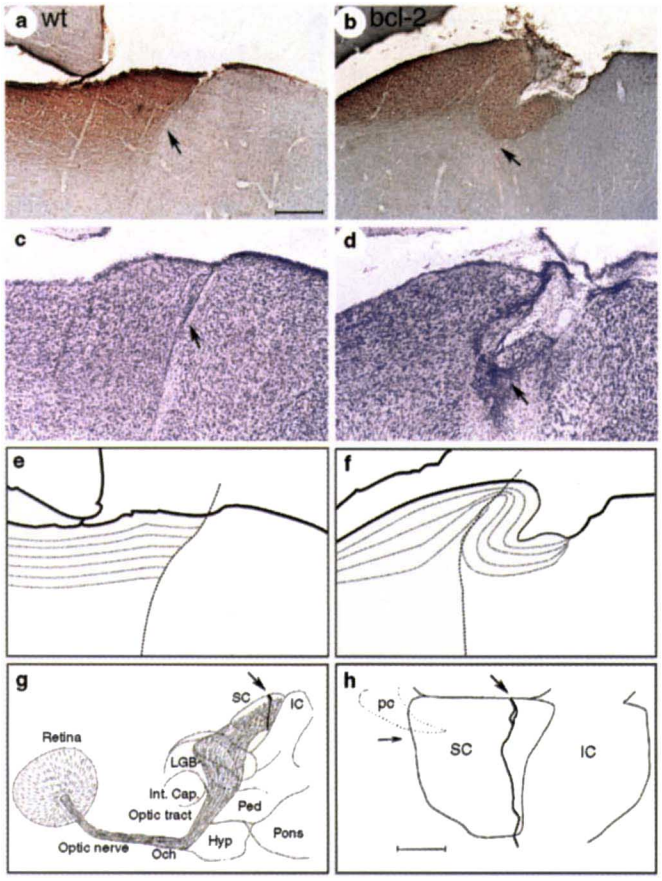

Figure 3 Expression of *bcl-2* in transgenic mice leads to regeneration of retinal axons after optic-tract transection *in vivo*. **a**, **b**, Photomicrographs of anterogradely labelled retinotectal axons after optic-tract transection; **c**, **d**, staining of adjacent brain sections with cresyl violet; **e**, **f**, drawings of **a**–**d**, using dotted lines to highlight the path of retinotectal projections and the bold dashed line for the lesion. **g**, A reconstructed view of the rodent optic nerve and the tract. **h**, A reconstructed top view of the superior colliculus from one case. Note that in wild-type (wt) animals (**a**), labelled axons do not cross the lesion site; those from *bcl-2* transgenic mice (bcl-2) (**b**) regenerate across the lesion site and enter the caudal tectum. Arrows point to the lesion site; additional arrows in **h** indicate the position of the sagittal sections (**b**, **d**). Abbreviations: Hyp, hypothalamus; IC, inferior colliculus; Int. Cap., internal capsule; LGB, lateral geniculate body; Och, optic chiasm; pc, posterior commissure; Ped, cerebral peduncle; SC, superior colliculus. Scale bar, 200 μm.

the RGC layer ($n = 3$) (Fig. 1c); at E18, in parallel with the onset of regenerative failure in culture, the expression of *bcl-2* decreased to an undetectable level ($n = 3$) (Fig. 1d).

To determine whether *bcl-2* is required for the growth of retinal axons, we studied a loss-of-function animal model: mice genetically deficient in *bcl-2* (ref. 6). Co-cultures were prepared from E15 embryos that contained wild-type, heterozygous and *bcl-2*-deficient mice. At this stage, retinal explants of wild-type animals showed robust neurite outgrowth. However, in cultures prepared from heterozygous animals, the number of labelled retinal axons was reduced by about 50% (62 ± 8, $n = 20$); in those from homozygous animals, the number was reduced by about 80% (22 ± 4, $n = 7$) (Fig. 2a). To exclude the possibility that tectal tissues from mutant mice may affect axonal growth of RGCs, retinal explants from each animal were also co-cultured with the tectum from a wild-type, heterozygous or homozygous animal. There was no significant difference between groups of retinae co-cultured with tecta from wild-type and mutant mice (data not shown). The number of retinal axons from cultures of mice containing the homozygous *bcl-2* mutation was equivalent to that of wild-type mice at E18, when most RGCs failed to grow axons into tectum. To examine further whether the differences in axonal growth observed were accounted for by the difference in the number of neurons in the retinae, RGC numbers were assessed in the retinae of six mice: two wild-type, three *bcl-2* heterozygous, and one *bcl-2* homozygous. The mean numbers of RGCs counted in 200-μm retinal segments in our sections were 89.3 ± 1.1, 89.0 ± 0.7 and 87.1, respectively. The number of RGCs among 28 sections of each animal showed little variation (s.e.m., 3.5–6.5% of mean within each retina). The size of the eyeball (diameter, 0.83–0.85 mm) and the diameter of the RGCs of these mice were very similar, so the differences in axonal growth observed with wild-type mice and mice mutated for *bcl-2* cannot be accounted for by differences in the number of RGCs.

Because loss of Bcl-2 function represses axonal growth, we wished to determine whether overexpression of *bcl-2* in adult retinae is sufficient for retention of the ability for retinal axon regeneration. Therefore, we analysed mice transgenic for the *bcl-2* gene driven by the neuron-specific enolase promoter[7,8]; our study was performed on line 73 of these transgenic mice. We examined co-cultures of retinae and tecta derived from animals aged E14 to postnatal day 5 (P5, where P0 is the day of birth), which covered the period before and after regenerative failure normally occurs. As previously described, retinal explants from each mouse were co-cultured with tecta of wild-type or transgenic mice. Starting at E18, retinal explants from wild-type mice exhibited a failure of RGC axon elongation ($n = 15$) (Fig. 2c), regardless of whether they were confronted with wild-type or transgenic tectal tissues. The number of labelled retinal axons decreased 10-fold in comparison to E16 retinal explants. In contrast, when retinae were derived from *bcl-2* transgenic animals, all retinal explants, collected from animals aged E14 to P5, showed extensive fibre outgrowth ($n = 35$) (Fig. 2c). No difference was observed in the number of retinal axons that invaded tectal slices derived from wild-type and *bcl-2* transgenic mice (data not shown). Furthermore, it has been reported that, in the retinae of the transgenic mouse line 73, *bcl-2* is detected primarily in RGCs[7]. We therefore conclude that constitutive expression of *bcl-2* in RGCs, rather than in the CNS environment of the axon, overcomes regenerative failure of retinal axons in the perinatal period.

RGCs derived from *bcl-2* transgenic mice retained the ability to grow axons throughout their lifespan. Extensive neurite outgrowth was observed from adult retinal explants of transgenic mice when they were co-cultured with E16 tectal slices ($n = 10$); the number of labelled retinal axons averaged 96.3 ± 15.3, almost equivalent to the number obtained from an E16 retinotectal co-culture. However, when the adult retinae were confronted with adult tectal tissues, little axonal growth was achieved ($n = 13$) (Fig. 2b). We do not yet know why adult tectal tissue prevented axon regeneration from retinae of mice overexpressing *bcl-2*. It is likely that adult CNS contains inhibitory molecules, such as myelin-associated inhibitory proteins, that are absent in embryonic tissues[9] or that they express low levels of neurotrophic factors that are required for the regrowth of retinal axons. Despite these factors, the normal embryonic retinae can grow axons into adult tectum[2], indicating that important factors additional to *bcl-2* are probably involved. In any case, we can conclude that *bcl-2* is central to the regulation of the intrinsic genetic program for retinal axonal growth, and that *bcl-2* is essential, but not sufficient, for the regeneration of retinal axons in mature CNS.

We then investigated regeneration of retinal axons *in vivo*. Young pups (P4) obtained from the mating of males heterozygous for the *bcl-2* transgene and C57BL/6J females received a unilateral transection of the optic tract at the mid-tectal level (Fig. 3c, d, g, h). Axonal regrowth was assessed by tracing the retinal projection fibres with cholera toxin B-subunit (CT-B)[10]. To visualize the lesion site,

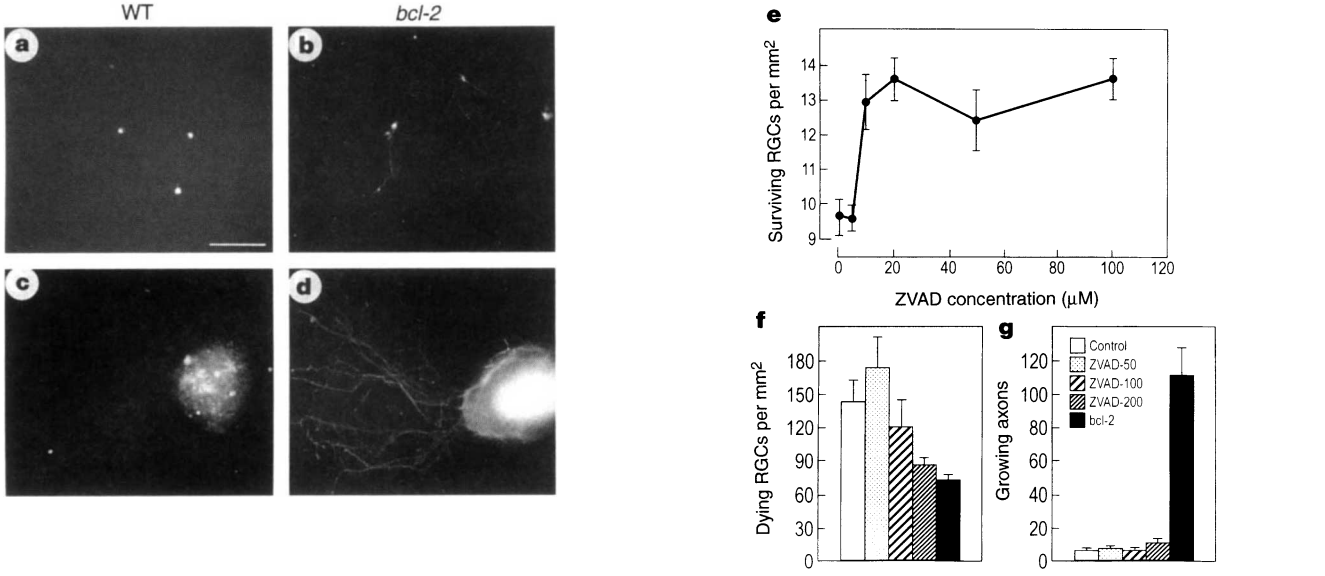

Figure 4 ZVAD, although sufficient to prevent the death of RGCs, is not sufficient to promote axonal growth. **a**–**d**, Epifluorescence photomicrographs of DiI-labelled RGCs obtained from dissociated (**a**, **b**) and explant (**c**, **d**) retinal cultures using tissues from P2 wild-type (**a**, **c**) or transgenic (**b**, **d**) mice. RGCs from wild-type mice (wt) surviving in ZVAD-treated cultures are round and devoid of neurites. In contrast, RGCs from transgenic mice (*bcl-2*) extend long axons in culture. **e**, Surviving RGCs in dissociated retinal cell cultures treated with different doses of ZVAD; doses from 0 to 200 μM were tested. **f**, Quantification of cell death in retinal explants from ZVAD-treated retinotectal co-cultures: three doses of ZVAD (50, 100 and 200 M) were examined, and cultures were prepared from P2 wild-type animals. **g**, Quantification of retinal axon growth in co-culture experiments parallel to those in **f**. By increasing the concentration of ZVAD, the number of dying cells in retinal explants decreased, but the number of growing axons did not change significantly. All data represent at least 3 replicated experiments. Scale bar, 200 μm.

alternate sagittal sections of these brains were collected for cresyl violet staining and reconstructed in three-dimensions with the Neurotrace program. In wild-type mice, the retinotectal projection was restricted to the tissue proximal to the lesion site ($n = 5$) (Fig. 4a, c, e). In contrast, axotomized retinal axons in transgenic mice grew in large numbers across the lesion site and innervated the tectum caudal to the injury ($n = 6$) (Fig. 3b, d, f). Remarkably, in three transgenic mice, the lesion produced a large, impassable gap in the superficial superior colliculus, but the axons were observed to go around the gap, and then pass straight through the lesion site below the gap on their way to the target tissue (Fig. 3b, f), without the addition of any bridging material or neurotrophic factors. Regenerating axons reached the posterior border of the superior colliculus. Our three-dimensional reconstruction showed that axons innervated the entire area of superior colliculus caudal to the lesion site. No axons were observed to invade the inferior colliculus. Although it has been documented that larger numbers of neurons and axons were found in these mutants than those in wild-type animals[7,8], the retinofugal projections to the lateral geniculate body and superior colliculus of transgenic mice seemed to be very similar to those in normal wild-type mice (data not shown). These results demonstrate that *bcl-2* promotes retinal axon regeneration *in vivo*.

It should be emphasized that the above experiment was designed to result in a minimal amount of tissue damage, so that large numbers of RGCs in wild-type mice survived after injury; however, they were unable to regenerate severed axons. Similar observations suggesting a dissociation of neuronal survival and axonal regrowth after axotomy have previously been reported[11].

The anti-apoptotic function of Bcl-2 is well established[12,13], so it is important to establish whether its growth-promoting activity is simply an indirect consequence of increased cell survival. It has been suggested that Bcl-2 suppresses apoptosis by impairing the activity of interleukin-1β-converting enzyme (ICE)[14–17], a cysteine protease thought to be essential in the apoptotic process in vertebrates[14–16]. To test the relationship between the functions of axonal growth and cell survival, we added the irreversible ICE-like protease inhibitor ZVAD (Z-Val-Ala-Asp-CH_2F; Enzyme Systems Products)[16,18] in a dissociated cell culture system that allows visualization of single cell morphology. We prepared cultures from retinae of P2 pups, and RGCs were prelabelled by injecting DiI into the tectum of P0 pups. We plated 10^5 cells that contained 4.8% (averaging 4,800) RGCs in each well of 24-well plates. Treatment with ZVAD at a concentration of 10 μM or above effectively reduced RGC death after 2 days in culture. The number of surviving RGCs was increased from 25% (without ZVAD) to about 40% (Fig. 4e). With this concentration of ZVAD, cultures derived from wild-type and *bcl-2* transgenic mice contained equal numbers of surviving RGCs (data not shown). Nevertheless, labelled RGCs from wild-type animals were round and devoid of neurites in culture ($n = 36$ cultures) (Fig. 4a, c), whereas RGCs derived from *bcl-2* transgenic mice ($n = 24$ cultures) exhibited extensive axonal outgrowth (Fig. 4b, d). Note that this occurs in the absence of any neurotrophic factors added to the culture medium. To test the possibility that wild-type RGCs do not grow neurites because of a shortage of neurotrophic factors, we added BDNF and NT-3 to the culture medium. These factors increased the number of surviving RGCs, as they had *in vivo*[19], but the proportion of RGCs with regenerating axons among the total number of surviving RGCs remained unchanged from that of the untreated control (data not shown).

We also tested the effect of the ICE inhibitor in our explant co-culture system with tissue prepared from wild-type P2 mice. Treatment with ZVAD reduced the extent of cell death in retinal explants (Fig. 4f). As we found in dissociated retinal cultures, 200 μM ZVAD protected cells from death almost as well as did *bcl-2* in the transgenic mouse ($n = 6$) (Fig. 4f); however, the number of axons that invaded tectal slices was 10-fold less in cultures from wild-type animals than in those from *bcl-2* transgenic mice (Fig. 4g). Therefore, these experiments indicated that cell survival and axonal growth are two distinct activities of RGCs; Bcl-2, but not ICE inhibitors, supports both of these activities.

The dissociation between cell survival and axonal growth[20,21] is supported by our observations. First, the regenerative failure of

retinal axons and the decrease in Bcl-2 levels in RGCs occur earlier (at E18) than most programmed cell death (P1–P5)[22]. This corresponds with the observation that the expression pattern of *bcl-2* does not mirror recognized patterns of cell death in the CNS[23]; rather, it seems to correlate with cell differentiation and capacity for axonal outgrowth of neurons[23]. Second, before birth the densities of RGCs are similar in retinal explants from wild-type mice and mice transgenic or with null mutations for *bcl-2* (refs 7, 8, 24), yet these neurons exhibited drastic differences in the ability to grow axons in culture. This implies that the differences in axonal growth observed in culture were not accounted for by differences in the number of RGCs in their retinae. Finally, our experiments using ZVAD further demonstrated that ICE inhibitor, although sufficient to block cell death, is not sufficient to support axonal growth. These findings all suggest that Bcl-2 promotes axonal growth through a mechanism independent of its anti-apoptotic activity. However, we cannot exclude the possibility that, in *bcl-2* transgenic mice, a subpopulation of RGCs that possesses the ability to regrow its axons might be specifically rescued from death during development. The hypothesis of the growth-promoting function of *Bcl-2* is supported by our findings, but also needs to be further tested.

It has recently been shown that Bcl-2 promotes neurite sprouting by regulating neural differentiation *in vitro*[25]. It interacts with a member of the Ras family, R-*ras* p23 (ref. 26), and is co-immunoprecipitated with the serine/threonine-specific protein kinase Raf-1 (ref. 27). These molecules have been implicated as components of growth-factor-mediated signal-transduction pathways that regulate neurite outgrowth[28]. Whether Bcl-2 acts through these molecules to execute its growth-promoting activity should be examined.

In summary, our results indicate that Bcl-2 can act as a regulatory switch for a genetic programme that controls the growth of CNS axons. This finding strengthens the notion that, for most developing CNS neurons, the ability to extend axons is governed by an intrinsic developmental programme. It provides a basis for the design of new therapeutic strategies for treatment of brain and spinal injuries, as well as many neurodegenerative diseases. □

Methods

Retinotectal co-culture. Retinotectal co-cultures were prepared essentially as described[2]. Briefly, brains were dissected, and coronal slices through the superior colliculus were cut with a McIlwain tissue chipper at a thickness of 300 μm. Each retina was cut in half and abutted against a tectal slice. Tissues were placed on the microporous membrane of Millicell wells and maintained in NeuralBasal medium supplemented with B27 at 37 °C for 5 days. To exclude the possibility that tectal tissues from mutant mice may affect axonal growth of RGCs, we set up a series of parallel experiments in which one retinal explant of each mouse was confronted with the tectum from the same mouse, while the second retinal explant was placed against the tectum from another mouse. With this arrangement, retinal explants from each animal had the possibility of being co-cultured with the tectum from a *bcl-2* transgenic, wild-type, heterozygous or homozygous animal. Because mouse tails were collected after the animals had been killed for culturing, all the results were actually obtained and scored blind before the genotype was determined. The number of regenerating axons was sampled by applying four DiI crystals to each fixed retinal explant. Thus a small portion of RGCs in each explant was labelled. Data from each group were drawn from at least 6 explant cultures (equivalent to 24 samples). The co-cultures were stored in fixative for 2–4 weeks to allow diffusion of the dye, and labelled retinal axons were viewed with a fluorescence microscope (Nikon).

Quantification of RGC densities in retinae. The eyecups from E16 and E18 mice were dissected and sectioned at 10 μm on a cryostat. The total number of sections was recorded to measure the diameter of the eyeball. The sections were then stained with cresyl violet. For each eye, three sections, including one with the optic nerve head and two others that were 300 μm away from the centre section, were selected. Cells contained in the RGC layer were counted in 6–11 fields (200 μm long) to cover the full length of each section. Pyknotic cells were identified by the presence of condensed and darkly stained nuclei[5]. Results are presented as mean ± s.e.m.

Immunofluorescence staining. E16 or E18 mouse embryos were obtained by Caesarian section of timed-mated, wild-type mothers. Brains were removed and fixed in 4% paraformaldehyde overnight and cut into transverse sections 10 μm thick with a cryostat. Sections were blocked with PBS containing 2.5% normal goat serum, 2.5% fetal bovine albumin, and 0.3% Triton X-100 for 30 min at room temperature, and then incubated with affinity-purified primary antibody (hamster anti-mouse *bcl-2*, 1:50; PharMingen) at 4 °C overnight. Secondary antibody (FITC-conjugated goat antibody to hamster immunoglobulin, 1:200) was then applied to the slide for 2 h at room temperature. The slides were rinsed several times in PBS, mounted in Fluoremount G, and viewed with the fluorescence microscope.

Surgery. Mouse pups were obtained from matings of males heterozygous for the *bcl-2* transgene with C57BL/6J females. Four days after birth (P4), pups received a unilateral transection of the optic tract at the mid-tectal level. To be sure the axons had been cut, transection was made with a knife followed by transverse passage of a tungsten hook that was pulled deeply through the superficial layers of superior colliculus, reaching the surface of the central grey. Regeneration of the optic tract was assessed using anterograde tracing with CT-B 10 days after the transection. To visualize the axons, a DAB reaction was performed using a slightly modified version of a previous protocol[10]. Briefly, brains were cut into 50-μm sagittal sections; alternate sections were collected for cresyl violet staining, and remaining sections were incubated with primary antibody against CT-B at 4 °C for 96 h and then further processed with ABC elite kit (Vector). Sections were visualized with a Nikon microscope. Serial sections from one transgenic mouse were used for a three-dimensional reconstruction with MIT Neurotrace computer software to obtain a detailed assessment of the width and depth of the lesion, and of the size of the reinnervated superior colliculus. Mouse tails were scored blind before the genotype was determined.

Dissociated retinal cell cultures. Primary cultures of dissociated retinal cells were prepared from P2 wild-type or transgenic animals. RGCs were prelabelled by injecting DiI solution (25% in dimethyl formamide) into the tectal region bilaterally in P0 pups. Cells were plated in 24-cell wells treated with poly-L-lysine (10 μg ml^{-1} at 4 °C overnight) and coated with human merosin (0.2 μg ml^{-1} at room temperature for 2 h)[29]. We plated 10^5 cells that contained 4.8% (averaging 4,800) RGCs in each well. The numbers of retinal cells and RGCs were counted before plating, using a Nikon microscope equipped with phase-contrast and fluorescence illumination. RGCs were identified by DiI labelling, and were found to comprise, on average, 4.8% of retinal cells at this age. Cultures were maintained for 2 days in NeuralBasal medium supplemented with B27, and the number of surviving RGCs were counted after culturing. Trypan blue staining was used to examine the viability of RGCs[14]. Morphologically, cells undergoing apoptosis were distinguished by condensed chromatin and shrunken cell bodies[30]. Retinotectal co-cultures prepared from wild-type P2 mice have been described[2] and ZVAD was added to the culture medium at the time of plating. Cell death was detected by staining with the fluorescent dye Sytox green fluorescent dead-cell stain (Molecular Probes).

Received 20 August; accepted 18 December 1996.

1. Aubert, I., Ridet, J.-L. & Gage, F. *Curr. Opin. Neurobiol.* **5,** 625–635 (1995).
2. Chen, D. F., Jhaveri, S. & Schneider, G. E. *Proc. Natl Acad. Sci. USA* **92,** 7287–7291 (1995).
3. Shewan, D., Berry, M. & Cohen, J. *J. Neurosci.* **15,** 2057–2062 (1995).
4. Aigner, L. *et al. Cell* **83,** 269–278 (1995).
5. Perry, V. H., Henderson, Z. & Linden, R. *J. Comp. Neurol.* **219,** 3546–3568 (1983).
6. Veis, D. J., Sorenson, C. M., Shutter, J. R. & Korsmeyer, S. J. *Cell* **75,** 229–240 (1993).
7. Martinou, J.-C. *et al. Neuron* **13,** 1017–1030 (1994).
8. Dubois-Dauphin, M., Frankowski, H., Tsujimoto, Y., Huarte, J. & Martinou, J.-C. *Proc. Natl Acad. Sci. USA* **91,** 3309–3313 (1994).
9. Schnell, L. & Schwab, M. E. *Nature* **343,** 269–272 (1990).
10. Angelucci, A., Clascá, F. & Sur, M. *J. Neurosci. Methods* **65,** 101–112 (1996).
11. Misantone, L. J., Gershenbaum, M. & Murray, M. *J. Neurocytol.* **13,** 449–465 (1984).
12. Davies, A. M. *Trends Neurosci.* **18,** 355–358 (1995).
13. Korsmeyer, S. J. *Immunol. Today* **13,** 285–288 (1992).
14. Gagliardini, V. *et al. Science* **263,** 826–828 (1994).
15. Miura, M., Zhu, H., Rotello, R., Hartwieg, E. A. & Yuan, J. *Cell* **75,** 653–660 (1993).
16. Henkart, P. A. *Immunity* **4,** 195–201 (1996).
17. Nicholson, D. W. *et al. Nature* **376,** 37–43 (1995).
18. Fletcher, D. S. *et al. J. Interferon Cytokine Res.* **15,** 243–248 (1995).
19. Mansour-Robaey, S., Clarke, D. B., Wang, Y. C., Bray, G. M. & Aguayo, A. J. *Proc. Natl Acad. Sci. USA* **91,** 1632–1636 (1994).
20. Sagot, Y., Tan, S. A., Hammang, J. P., Aebischer, P. & Kato, A. C. *J. Neurosci.* **16,** 2335–2341 (1996).
21. Dusart, I. & Sotelo, C. *J. Comp. Neurol.* **347,** 211–232 (1994).
22. Young, R. W. *J. Comp. Neurol.* **229,** 362–373 (1984).
23. Merry, D. E., Veis, D. J., Hickey, W. F. & Korsmeyer, S. J. *Development* **120,** 301–311 (1994).
24. Michaelidis, T. M. *et al. Neuron* **17,** 75–89 (1996).

25. Zhang, K.-Z., Westberg, J. A., Hölttä, E. & Andersson, L. C. *Proc. Natl Acad. Sci. USA* **93,** 4504–4508 (1996).
26. Fernandez-Sarabia, M. J. & Bischoff, J. R. *Nature* **366,** 274–275 (1993).
27. Wang, H.-G. *et al. Oncogene* **9,** 2751–2756 (1994).
28. Greene, L. A. & Kaplan, D. R. *Curr. Opin. Neurobiol.* **5,** 579–587 (1995).
29. Meyer-Franke, A., Kaplan, M. R., Pfrieger, F. W. & Barres, B. A. *Neuron* **15,** 805–819 (1995).
30. Barres, B. A. *et al. Cell* **70,** 31–46 (1992).

Acknowledgements. We thank M. Wu for technical assistance; Y.-Q. Li for establishing the *bcl-2* transgenic mouse colony; and H. Steller, S. Jhaveri, L. Benowitz and J.-W. Han for critical comments on the manuscript. This work was supported by the Howard Hughes Medical Institute, the Shionogi Institute for Medical Science (S.T.) and an NEI-NIH grant (G.S.).

Competitive binding of α-actinin and calmodulin to the NMDA receptor

Michael Wyszynski, Jerry Lin, Anuradha Rao*, Elizabeth Nigh, Alan H. Beggs†, Ann Marie Craig* & Morgan Sheng

Howard Hughes Medical Institute and Department of Neurobiology, Massachusetts General Hospital and Harvard Medical School, Boston, Massachusetts 02114, USA
** Department of Cell and Structural Biology, University of Illinois, Urbana-Champaign, Illinois 61801, USA*
† Genetics Division, Children's Hospital and Harvard Medical School, Boston, Massachusetts 02115, USA

The mechanisms by which neurotransmitter receptors are immobilized at postsynaptic sites in neurons are largely unknown. The activity of NMDA (*N*-methyl-D-aspartate) receptors is mechanosensitive[1] and dependent on the integrity of actin[2], suggesting a functionally important interaction between NMDA receptors and the postsynaptic cytoskeleton. α-Actinin-2, a member of the spectrin/dystrophin family of actin-binding proteins, is identified here as a brain postsynaptic density protein that colocalizes in dendritic spines with NMDA receptors and the putative NMDA receptor-clustering molecule PSD-95. α-Actinin-2 binds by its central rod domain to the cytoplasmic tail of both NR1 and NR2B subunits of the NMDA receptor, and can be immunoprecipitated with NMDA receptors and PSD-95 from rat brain. Intriguingly, NR1-α-actinin binding is directly antagonized by Ca^{2+}/calmodulin. Thus α-actinin may play a role in both the localization of NMDA receptors and their modulation by Ca^{2+}.

NMDA receptors exist *in vivo* as heteromultimeric complexes consisting of the essential NR1 subunit coassembled with various subunits of the NR2 subfamily[3–8]. An association between NR2 subunits and the PSD-95/SAP90 family of synaptic proteins has been identified[9,10], but the nature of specific proteins that mediate NMDA receptor interaction with the postsynaptic actin cytoskeleton is not known. The carboxy-terminal intracellular domain of NR1 (Fig. 1) represents a potential target for intracellular anchoring molecules, especially as alternative splicing within this C-terminal region can affect the subcellular distribution of NR1(ref. 11).

A yeast two-hybrid screen of a human brain complementary DNA library was performed using as bait the C-terminal tail from the most abundant NR1 splice variant (NR1A)[12] (Fig. 1a, b). This C-terminal splice variant contains both C-terminal exon cassettes (termed C1 and C2) as well as the membrane-proximal region (here termed C0), and is thus referred to as C0-C1-C2 (Fig. 1, inset). The two-hybrid screen yielded multiple isolates of two distinct clones (A1.7 and A2.10) which interacted specifically with the C-terminal intracellular tail of NR1, but not with Shaker-type K^+ channel subunits or the AMPA-receptor subunit GluR1. Clone A1.7 interacted with the C0-C1-C2 but not with the C0-C2 C-terminal variant and encoded a new protein with weak homology to muscle myosin heavy chain (M.W. and J.L., unpublished observations). Clone A2.10 interacted with both the C0-C1-C2 and C0-C2 variants of NR1 and contained a 2.2-kilobase (kb) cDNA encoding the C-terminal two thirds of the human α-actinin-2 gene (Fig. 1a)[13]. The

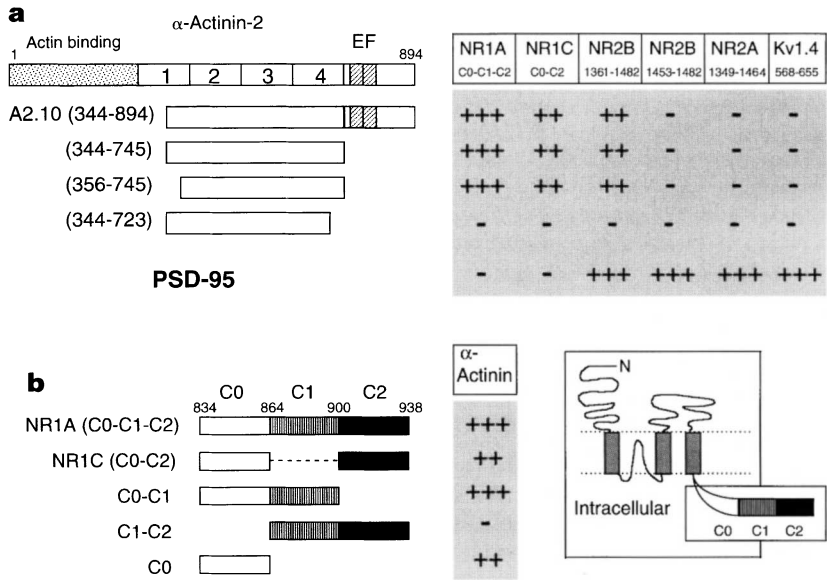

Figure 1 a, α-actinin-2 binds to the cytoplasmic tails of NR1 and NR2B through its central rod domain. Clone A2.10, and further deletion variants, are shown aligned under full-length α-actinin-2, in which the actin-binding domain, repeats 1–4 of the central rod domain, and EF hands are indicated. The interaction of α-actinin-2 constructs with the cytoplasmic tails of NR1, NR2B, NR2A and Kv1.4 are shown, as measured by the yeast two-hybrid assay. Numbers refer to amino-acid residues at the boundaries of each construct. Yeast two-hybrid interactions were semi-quantified on the basis of induction of the reporter genes *HIS3* and β-galactosidase[21]. **b**, The C0 segment of the NR1 C-terminal tail is necessary and sufficient for binding to α-actinin-2. Deletion constructs of the NR1 C-terminal tail were tested for interaction with α-actinin-2 (A2.10) by yeast two-hybrid assay. Numbers refer to the amino-acid residues at the boundaries of C0, C1 and C2 segments[25]. Inset, membrane topology of NR1. The intracellular tail consists of the membrane proximal segment C0, and C-terminal exon-segments C1 and C2.